JGR Earth Surface

Supporting Information for

Controls on Physical and Chemical Denudation in a Mixed Siliciclastic-Carbonate Orogen

E. D. Erlanger[1,2], J. K. C. Rugenstein[3], A. Bufe[2], V. Picotti[1], and S. D. Willett[1]

[1]Department of Earth Science, ETH Zürich, Zürich, Switzerland

[2]GFZ, Telegrafenberg, Potsdam, Germany

[3]Department of Geosciences, Colorado State University, Fort Collins, CO 80521, USA

Contents of this file

Introduction

Text S1 in the supporting information justifies the exclusion of samples that show evidence for draining evaporite deposits, Text S2 describes the data used for the global denudation and weathering flux comparison, and Text S3 provides the equations used for calculating secondary carbonate precipitation. . Tables in the supporting information provide sample information, solute concentrations, or calculated metrics (e.g. saturation index) as a reference for figures included in the main text. Figures in the supporting information illustrate either aspects or justifications for the methods employed in this paper (Figures S2, S3, and S5), provide pictures of the lithologic units that we describe in the main text (Figures S1 and S6), or complement data presented in the text (Figure

S7). We note that none of the figures presented here are necessary for comprehending the main text.

Evaporite Weathering (Text S1)

In the absence of evaporite deposits, the total amounts of Ca^{2+} and Mg^{2+} in water samples reflect weathering of both silicates and carbonates. However, evaporites such as gypsum ($CaSO_4$) may represent another substantial source of dissolved, riverine Ca^{2+} (Meybeck, 1987). In carbonate catchments, the expected stoichiometric ratio of $(Ca + Mg)/HCO_3$ is 0.5 in pristine water (Sarin et al., 1989; Perrin et al., 2008). In the absence of evaporite deposits, calculated ratios along the Brahmaputra River are 1.09 ± 0.1 (Sarin et al., 1989), and between 1–2 for small catchments in France that were cultivated with nitrogen fertilizers (Perrin et al., 2008). The average $(Ca + Mg)/HCO_3$ ratio and 2σ errors for our river samples is 1.21 ± 0.32 (R^2 = 0.74), a value that indicates negligible Ca- and Mg-bearing evaporite sources. High concentrations of SO_4^{2-}, Na^+, and Ca^{2+} were found in three of the studied catchments (No. 3, 5, and 15). These rivers fell outside the average ratios of $(Ca + Mg)/HCO_3$ for all other catchments, consistent with observations of evaporite sources (halite and gypsum) in catchments 3 and 15 (Cortecci et al., 2008; Chiesi et al., 2010; Boschetti et al., 2011), and were therefore excluded from the weathering flux calculations (Figure S2).

Global Denudation and Weathering Flux Dataset Calculations (Text S2).

A variety of methods have been employed to calculate the associated denudation and physical erosion fluxes for the global dataset. Most estimates of physical erosion in these data are derived from stream sediment fluxes (Hodson et al., 2000; Millot et al., 2002; Picouet et al., 2002; Hosein et al., 2004; West et al., 2005). A small subset of studies have calculated denudation and physical erosion fluxes from detrital cosmogenic nuclides measured in river sediments (Galy and France-Lanord, 2001; West et al., 2005). In turn, chemical weathering fluxes are calculated using either annual average element budgets or spot chemistry measurements combined with annual discharge.

We compare our weathering data to studies that also calculated chemical weathering fluxes either from oxide concentrations of Ca^{2+}, Mg^{2+}, K^+, Na^+, and Si or from cation

concentrations. Note that for the purposes of comparison, we exclude the contribution of anions (CO_3) from our carbonate weathering flux calculation (Equation 6, main text), in order to be consistent with the methods used to calculate weathering fluxes in the global compilation. Most global data points were extracted from West et al. (2005), from which we estimate weathering fluxes using the "Total Cation Denudation Rates fluxes" (TCDR), combined with weathering estimates of Si from SiO_2 fluxes. We also recalculated weathering fluxes for datapoints from the Andes (Gaillardet et al., 1997) using the methods employed in this paper, and corrected the initial concentrations for atmospheric Cl^- inputs using the weighted average composition of rainwater in the Amazon basin (8.31 μmol/L) calculated by Gaillardet al. (1997).

Secondary Carbonate Precipitation Calculations (Text S3)

With calcite precipitation, enrichment of Sr^{2+} occurs, and (Sr/Ca) increases, such that :

$$\frac{[Sr^{2+}]}{[Ca^{2+}]} = \frac{[Sr^{2+}]_0}{[Ca^{2+}]_0} \gamma^{(kd-1)} \quad (1)$$

where $\frac{[Sr^{2+}]_0}{[Ca^{2+}]_0}$ reflects the initial ratio of Sr to Ca in the absence of secondary precipitation, kd is the partition coefficient for Sr, and γ is the fraction of primary calcite that remains in the water at the sampling site (Bickle et al., 2015). $(Sr^{2+}/Ca^{2+})_0$ is constrained from elemental ratios in silicate and carbonate bedrock, which form an endmember mixing line. To estimate the endmember composition of local bedrock, we use published geochemical data of bedrock samples in the Northern Apennines (Bracciali et al., 2007; Dinelli et al., 1999). The carbonate endmember is defined as the inferred Sr/Ca content when Na/Ca equals zero, since carbonates are assumed to have negligible Na^+ (Bickle et al., 2015). We estimate the endmember mixing line for each lithology using bulk major ions and the trace element composition of sandstones from the the Marnoso Arenacea Unit (Figure 8a) and the Macigno-Cervarola Unit (Figure 8b) (Dinelli et al., 1999), and from the IntL Unit (Figure 8c) and the ExtL Unit (Figure 8d) (Bracciali et al., 2007). We have no constraints on the bedrock composition of the Epiligurian Unit. However, in

most cases the Epiligurian Unit represents deposition in satellite basins that were coeval with and coupled with the deposition of the Tertiary Foredeep Units (Ricci Lucchi, 1986a), so we expect that the composition of these units should be similar.

The best-fit endmember mixing lines through all data points for each lithologic unit is described by the equation:

$$\frac{\mathbf{1000}*[\mathbf{Sr^{2+}}]}{[\mathbf{Ca^{2+}}]} = \mathbf{a} + \mathbf{b}\ \frac{[\mathbf{Na^{+}}]}{[\mathbf{Ca^{2+}}]} \tag{2}$$

where a and b are the intercept and slope of the fit. Samples that have not experienced secondary calcite precipitation should fall on this line (uncorrected samples, Figure 8). Similarly, samples before secondary precipitation fall on that line. The amount of secondary precipitation is calculated as the deviation of the solute samples from the bedrock mixing line. We can rearrange equation (3) to solve for $\frac{[\mathbf{Sr^{2+}}]_0}{[\mathbf{Ca^{2+}}]_0}$

$$\frac{[\mathbf{Sr^{2+}}]_0}{[\mathbf{Ca^{2+}}]_0} = \frac{[\mathbf{Sr^{2+}}]}{[\mathbf{Ca^{2+}}]}\boldsymbol{\gamma}^{(\mathbf{1-kd})} \tag{3}$$

Moreover, we have from equation (2), the definition of $\boldsymbol{\gamma}$, and the assumption that the concentration of sodium does not change:

$$\frac{\mathbf{1000\ x}\ [\mathbf{Sr^{2+}}]_0}{[\mathbf{Ca^{2+}}]_0} = \mathbf{a} + \mathbf{b}\frac{[\mathbf{Na^{+}}]_0}{[\mathbf{Ca^{2+}}]_0} = \mathbf{a} + \mathbf{b}\frac{[\mathbf{Na^{+}}]}{[\mathbf{Ca^{2+}}]}\boldsymbol{\gamma} \tag{4}$$

Combining equations (3), and (4), we can minimize the following equation numerically for γ:

$$\frac{\mathbf{1000\ x}\ [\mathbf{Sr^{2+}}]}{[\mathbf{Ca^{2+}}]} * \boldsymbol{\gamma}^{(\mathbf{1-kd})} - \mathbf{a} - \mathbf{b}\frac{[\mathbf{Na^{+}}]}{[\mathbf{Ca^{2+}}]}\boldsymbol{\gamma} = \mathbf{0} \tag{5}$$

Samples were corrected for secondary calcite precipitation using a partition coefficient of k = 0.05. Previous studies suggest that the acceptable range of values for k is 0.02-0.2 (Tesoriero and Pankow, 1996; Gabitov and Watson, 2006; Nehrke et al., 2007), so we additionally performed the correction using the two endmember k values (k = 0.02 and k = 0.2), in order to assess the variability in the adjusted [Ca^{2+}] concentrations (Figure S5).

Using a lower k value results in a smaller correction to [Ca^{2+}], so the value used for our correction (k = 0.05) could be interpreted as a minimum; however, regardless of the k value used, the resulting correction to the original [Ca^{2+}] concentrations is substantial.

References

Bickle, M.J., Tipper, E., Galy, A., Chapman, H., and Harris, N., 2015, On discrimination between carbonate and silicate inputs to Himalayan rivers: American Journal of Science, v. 315, p. 120–166, doi:10.2475/02.2015.02.

Boschetti, T., Cortecci, G., Toscani, L., and Iacumin, P., 2011, Sulfur and oxygen isotope compositions of Upper Triassic sulfates from northern Apennines (Italy): Paleogeographic and hydrogeochemical implications: Geologica Acta, v. 9, p. 129–147, doi:10.1344/105.000001690.

Bracciali, L., Marroni, M., Pandolfi, L., Rocchi, S., Arribas, J., Critelli, S., and Johnsson, M.J., 2007, Geochemistry and petrography of Western Tethys Cretaceous sedimentary covers (Corsica and Northern Apennines): from source areas to configuration of margins: Special Paper of the Geological Society of America, v. 420, p. 73.

Chiesi, M., Waele, J. De, and Forti, P., 2010, Origin and evolution of a salty gypsum / anhydrite karst spring : the case of Poiano (Northern Apennines , Italy): , p. 1111–1124, doi:10.1007/s10040-010-0576-2.

Cortecci, G., Dinelli, E., Boschetti, T., Arbizzani, P., Pompilio, L., and Mussi, M., 2008, The Serchio River catchment, northern Tuscany: Geochemistry of stream waters and sediments, and isotopic composition of dissolved sulfate: Applied Geochemistry, v. 23, p. 1513–1543, doi:10.1016/j.apgeochem.2007.12.031.

Dinelli, E., Lucchini, F., Mordenti, A., and Paganelli, L., 1999, Geochemistry of Oligocene-Miocene sandstones of the northern Apennines (Italy) and evolution of chemical features in relation to provenance changes: Sedimentary Geology, v. 127, p. 193–207, doi:10.1016/S0037-0738(99)00049-4.

Emberson, R., Galy, A., and Hovius, N., 2018, Weathering of Reactive Mineral Phases in Landslides Acts as a Source of Carbon Dioxide in Mountain Belts: Journal of Geophysical Research: Earth Surface, p. 2695–2713, doi:10.1029/2018JF004672.

Gabitov, R.I., and Watson, E.B., 2006, Partitioning of strontium between calcite and fluid: Geochemistry, Geophysics, Geosystems, v. 7.

Gaillardet, J., Dupre, B., Allegre, C.J., and Négrel, P., 1997, Chemical and physical denudation in the Amazon River Basin: Chemical geology, v. 142, p. 141–173.

Galy, A., and France-Lanord, C., 2001, Higher erosion rates in the Himalaya: Geochemical constraints on riverine fluxes: Geology, v. 29, p. 23–26.

Garzanti, E., Canclini, S., Moretti Foggia, F., and Petrella, N., 2002, Unraveling magmatic and orogenic provenances in modern sands: the back-arc side of the Apennine thrust-belt (Italy): Journal of Sedimentary Research, v. 72, p. 2–17, doi:10.1306/051801720002.

Garzanti, E., Scutellà, M., and Vidimari, C., 1998, Provenance from ophiolites and oceanic allochtons: Modern beach and river sands from Liguria and the northern Apennines (Italy): Ofioliti, v. 23, p. 65–82, doi:10.4454/ofioliti.v23i2.2.

Hodson, A., Tranter, M., and Vatne, G., 2000, Contemporary rates of chemical denudation and atmospheric CO2 sequestration in glacier basins: an Arctic perspective: Earth Surface Processes and Landforms, v. 25, p. 1447–1471.

Hosein, R., Arn, K., Steinmann, P., and Adatte, T., 2004, Carbonate and silicate weathering in two presently glaciated, crystalline catchments in the Swiss Alps: Geochimica et Cosmochimica Acta, v. 68, p. 1021–1033.

Jacobson, A.D., Blum, J.D., and Walter, L.M., 2002, Reconciling the elemental and Sr isotope composition of Himalayan weathering fluxes: Insights from the carbonate geochemistry of stream waters: Geochimica et Cosmochimica Acta, v. 66, p. 3417–3429, doi:10.1016/S0016-7037(02)00951-1.

Meybeck, M., 1987, Global chemical weathering of surficial rocks estimated from river dissolved loads: American journal of science, v. 287, p. 401–428.

Millot, R., Gaillardet, J., Dupré, B., and Allègre, C.J., 2002, The global control of silicate weathering rates and the coupling with physical erosion: New insights from rivers of the Canadian Shield: Earth and Planetary Science Letters, v. 196, p. 83–98, doi:10.1016/S0012-821X(01)00599-4.

Nehrke, G., Reichart, G.-J., Van Cappellen, P., Meile, C., and Bijma, J., 2007, Dependence of calcite growth rate and Sr partitioning on solution stoichiometry: non-Kossel crystal growth: Geochimica et Cosmochimica Acta, v. 71, p. 2240–2249.

Perrin, A.S., Probst, A., and Probst, J.L., 2008, Impact of nitrogenous fertilizers on carbonate dissolution in small agricultural catchments: Implications for weathering CO2 uptake at regional and global scales: Geochimica et Cosmochimica Acta, v. 72, p. 3105–3123, doi:10.1016/j.gca.2008.04.011.

Picouet, C., Dupré, B., Orange, D., and Valladon, M., 2002, Major and trace element

geochemistry in the upper Niger river (Mali): physical and chemical weathering rates and CO2 consumption: Chemical Geology, v. 185, p. 93–124.

Ricci Lucchi, F., 1986, The Oligocene to Recent Foreland Basins of the Northern Apennines, *in* Allen, A. and Homewood, P. eds., Foreland Basins, Blackwell Scientific Oxford, Wiley Online Books, p. 105–139, doi:doi:10.1002/9781444303810.ch6.

Sarin, M.M., Krishnaswami, S., Dilli, K., Somayajulu, B.L.K., and Moore, W.S., 1989, Major ion chemistry of the Ganga-Brahmaputra river system: Weathering processes and fluxes to the Bay of Bengal: Geochimica et Cosmochimica Acta, v. 53, p. 997–1009, doi:10.1016/0016-7037(89)90205-6.

Tesoriero, A.J., and Pankow, J.F., 1996, Solid solution partitioning of Sr2+, Ba2+, and Cd2+ to calcite: Geochimica et Cosmochimica Acta, v. 60, p. 1053–1063.

West, A.J., Galy, A., and Bickle, M., 2005, Tectonic and climatic controls on silicate weathering: Earth and Planetary Science Letters, v. 235, p. 211–228, doi:10.1016/j.epsl.2005.03.020.

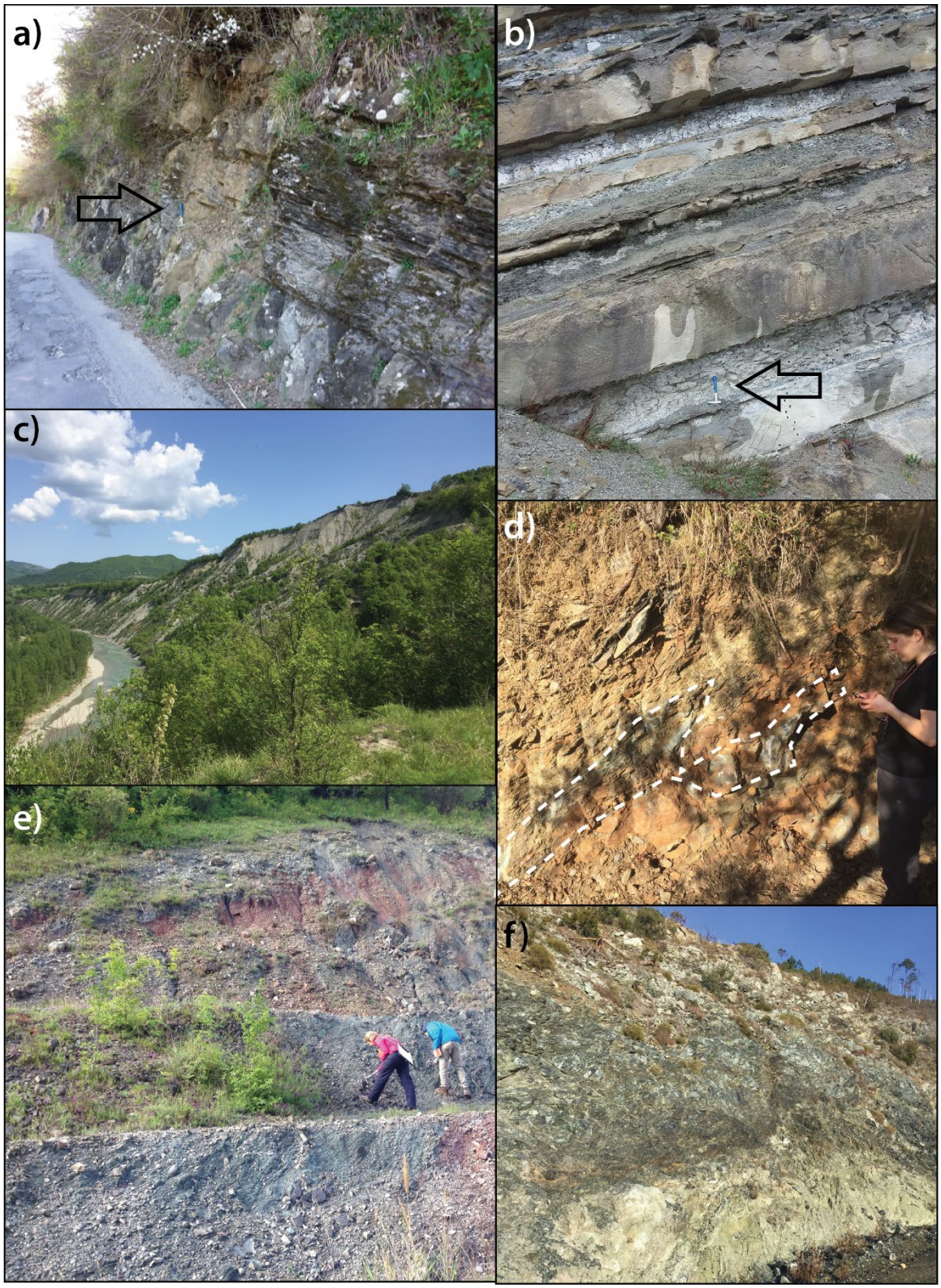

Figure S1. *Field examples of lithologies observed in the Northern Apennines. a) sandstones of the Macigno Unit, b) Interbedded sandstone and marls of the Marnoso Arenacea Unit, c) sandstone of the Epiligurian Unit (background), d) shale and limestone beds (white, dashed outline) and f)*

serpentinite of the Internal Ligurian Unit, and e) scaly clays of the External Ligurian Unit. Black arrows in a) and b) indicate rock hammers for scale.

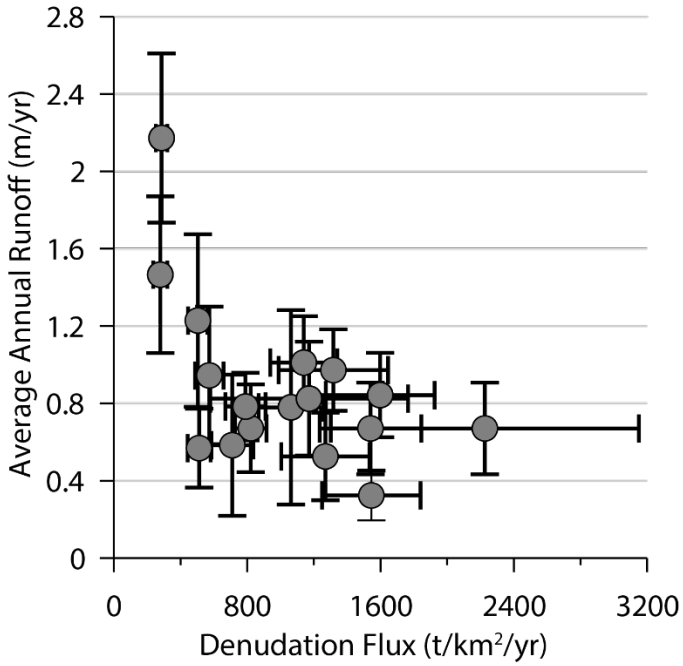

Figure S2. *Denudation fluxes plotted against annual runoff estimates averaged over the last five available years of data.*

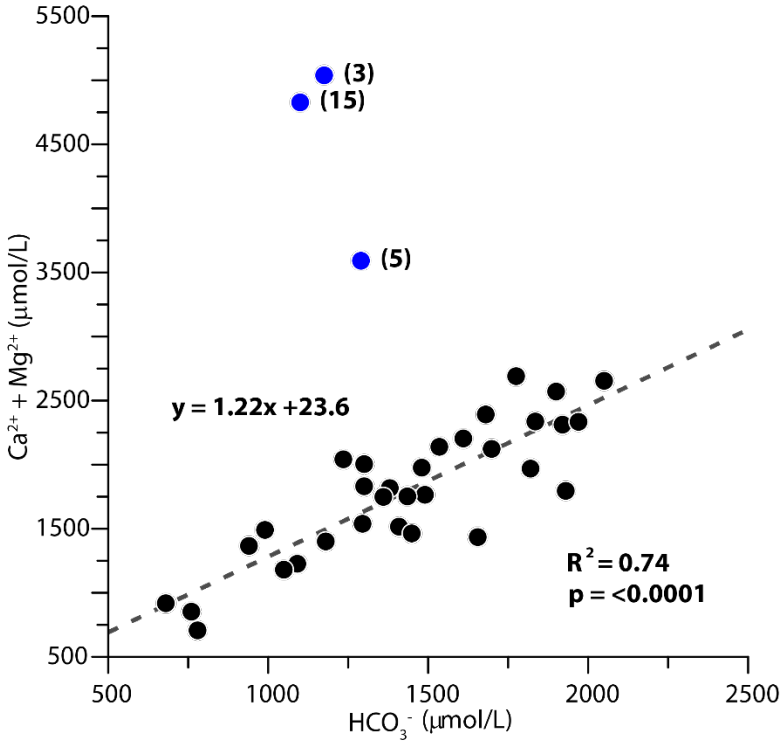

Figure S3. *Plot of HCO_3 against Ca + Mg. Linear regression (dashed line) and R^2 statistic apply only to black data points. Outlier data points are illustrated as blue circles; numbers correspond to river numbers shown in Figure 1a.*

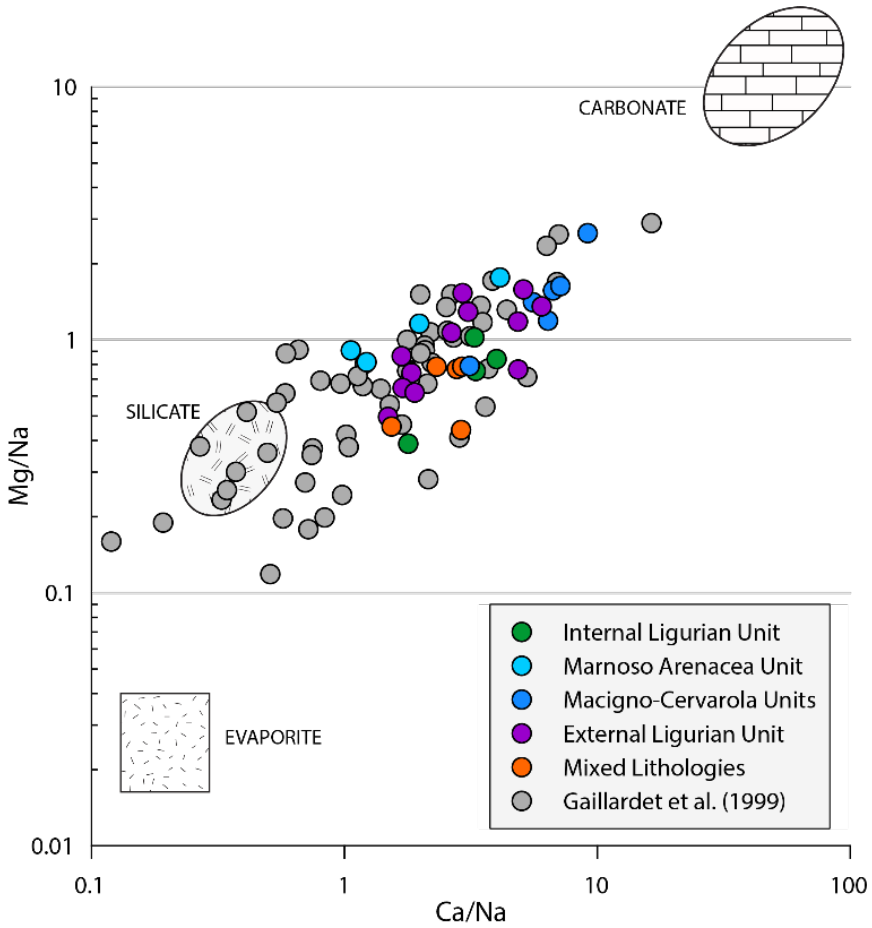

Figure S4. *Mixing diagram comparing ratios of Ca/Na and Mg/Na for different lithologies in the Northern Apennines (colored circles) with Gaillardet et al. (1999) global dataset (gray circles) and endmember compositions for carbonate, silicate, and evaporites.*

Catchment Number	Name	Locality	Sample Number	Latitude	Longitude	Sampling Date	Ca^{2+} (µmol/L)	Mg^{2+} (µmol/L)	Na^{+} (µmol/L)	K^{+} (µmol/L)	TDS_{Total} (µmol/L)	TDS_{Carb} (µmol/L)	TDS_{Sil} (µmol/L)	% Change TDS_{Total}
2	Lima	Borgo a Mozzano	1	43.999°	10.554°	7/15/2018	1150 ± 34	295 ± 15	384 ± 15	14 ± 1	1919 ± 42	1214 ± 38	705 ± 17	2.18
4	Serchio	Filicaia	1	44.137°	10.374°	7/15/2018	1648 ± 49	310 ± 16	269 ± 11	16 ± 1	2349 ± 54	1797 ± 52	552 ± 14	1.78
5	Magra	Aulla	1	44.187°	9.926°	3/20/2018	1144 ± 34	176 ± 9	413 ± 17	14 ± 1	1864 ± 41	1072 ± 36	792 ± 19	2.24
6	Vara	Piana Battolla	1	44.192°	9.858°	3/20/2018	653 ± 20	153 ± 8	213 ± 9	9 ± 1	1165 ± 25	678 ± 21	487 ± 12	3.59
6	Vara	Piana Battolla	2	44.190°	9.858°	7/15/2018	1131 ± 34	362 ± 18	362 ± 14	16 ± 1	1991 ± 43	1275 ± 39	715 ± 18	2.10
7	Entella	Carasco	1	44.351°	9.362°	3/20/2018	1137 ± 34	251 ± 13	661 ± 26	19 ± 1	1167 ± 25	756 ± 23	410 ± 10	3.59
7	Entella	Carasco	2	44.351°	9.362°	7/15/2018	718 ± 22	155 ± 8	194 ± 8	4 ± 0	2186 ± 48	992 ± 38	1194 ± 29	1.91
8	Scrivia	Serravalle Scrivia	1	44.719°	8.860°	3/18/2018	1510 ± 45	239 ± 12	323 ± 13	15 ± 1	2178 ± 50	1556 ± 47	622 ± 15	1.92
9	Staffora	Godiasco	1	44.893°	9.057°	7/15/2018	1375 ± 41	718 ± 36	842 ± 34	62 ± 4	3252 ± 69	1588 ± 57	1664 ± 40	1.29
10	Trebbia	Rivergaro	1	44.908°	9.590°	3/22/2018	1365 ± 41	337 ± 17	294 ± 12	12 ± 1	2112 ± 47	1526 ± 45	586 ± 15	1.98
10	Trebbia	Rivergaro	2	44.909°	9.589°	7/15/2018	1322 ± 40	449 ± 22	918 ± 37	29 ± 2	2868 ± 62	1220 ± 48	1648 ± 40	1.46
11	Nure	Vigolzone	1	44.882°	9.653°	3/21/2018	1771 ± 53	754 ± 38	591 ± 24	28 ± 2	3277 ± 72	2170 ± 66	1107 ± 28	1.28
11	Nure	Lugherzano	1	44.828°	9.617°	7/15/2018	1408 ± 42	750 ± 38	498 ± 20	36 ± 2	2891 ± 63	1860 ± 58	1032 ± 26	1.45
12	Taro	Ramiola	1	44.698°	10.093°	3/21/2018	1462 ± 44	461 ± 23	299 ± 12	28 ± 2	2347 ± 52	1744 ± 50	603 ± 15	1.78
12	Taro	Ramiola	2	44.697°	10.094°	7/15/2018	1369 ± 41	562 ± 28	535 ± 21	47 ± 3	2649 ± 57	1610 ± 51	1040 ± 25	1.58
13	Baganza	Calestano	1	44.605°	10.120°	3/21/2018	1846 ± 55	420 ± 21	317 ± 13	25 ± 2	2714 ± 62	2076 ± 60	638 ± 16	1.54
13	Baganza	Calestano	2	44.606°	10.123°	7/15/2018	1218 ± 37	501 ± 25	686 ± 27	33 ± 2	2562 ± 55	1307 ± 46	1255 ± 31	1.63
14	Parma	Pastorello	1	44.569°	10.237°	7/15/2018	1280 ± 38	426 ± 21	699 ± 28	32 ± 2	2519 ± 55	1287 ± 45	1233 ± 31	1.66
15	Enza	San Polo d'Enza	1	44.627°	10.413°	7/15/2018	1439 ± 43	557 ± 28	873 ± 35	50 ± 4	3008 ± 66	1472 ± 53	1536 ± 38	1.39
17	Panaro	Marano sul Panaro	1	44.420°	10.925°	7/4/2017	1327 ± 40	458 ± 23	594 ± 24	46 ± 3	2506 ± 54	1429 ± 47	1077 ± 26	1.67
18	Reno	Marzabotto	1	44.338°	11.213°	5/1/2017	1148 ± 34	323 ± 16	431 ± 17	18 ± 1	1955 ± 43	1212 ± 39	743 ± 19	2.14
18	Reno	Scuola	1	44.362°	11.257°	5/3/2017	1597 ± 48	480 ± 24	1069 ± 43	45 ± 3	3306 ± 73	1436 ± 56	1870 ± 46	1.27
18	Reno	Poretta Terme	1	44.100°	10.962°	5/4/2017	1020 ± 31	237 ± 12	153 ± 6	8 ± 1	1503 ± 34	1166 ± 33	337 ± 9	2.78
18	Reno	Sibano	1	44.317°	11.185°	5/5/2017	1113 ± 33	305 ± 15	398 ± 16	55 ± 4	1916 ± 41	1178 ± 37	738 ± 18	2.18
18	Reno	Lentula	1	44.079°	11.051°	5/5/2017	831 ± 25	200 ± 10	135 ± 5	14 ± 1	1287 ± 29	949 ± 27	338 ± 9	3.25
18	Reno	Limentrella di Treppio	1	44.085°	11.044°	5/5/2017	995 ± 30	294 ± 15	118 ± 5	89 ± 6	1745 ± 38	1218 ± 34	527 ± 17	2.40
18	Reno	Castello di Sambuca	1	44.104°	10.998°	5/5/2017	837 ± 25	217 ± 11	162 ± 6	83 ± 6	1523 ± 32	957 ± 28	566 ± 16	2.75
19	Senio	Casola Valsenio	1	44.227°	11.632°	7/15/2018	1390 ± 42	1218 ± 61	1350 ± 54	76 ± 5	4152 ± 98	1798 ± 78	2354 ± 60	1.01
20	Lamone	Biforco	1	44.065°	11.601°	7/15/2018	1433 ± 43	857 ± 43	748 ± 30	47 ± 3	3215 ± 71	1842 ± 63	1373 ± 35	1.30
21	Montone	Davadola	1	44.121°	11.885°	7/15/2018	1395 ± 42	951 ± 48	1174 ± 47	72 ± 5	3701 ± 84	1641 ± 67	2059 ± 52	1.13
21	Montone	San Benedetto	1	43.982°	11.689°	7/15/2018	940 ± 28	415 ± 21	242 ± 10	38 ± 3	1714 ± 38	1210 ± 36	504 ± 13	2.44

Table S1. *Elemental Concentrations and TDS calculations using a local precipitation correction for rainwater inputs. "% Change TDS_{Total}" reflects the percent difference between using global seawater ratios versus local precipitation ratios to perform the correction.*

	River/Location	Latitude	Longitude	Basin Area (km^2)	% Carbonate Sand (250-500 µm)	L_c grain counts	Avg Size of L_c grains (µm)
1	Bisenzio	43.9278°	11.1258°	149	28	NA	NA
2	Lima	43.9993°	10.5539°	317	20	NA	NA
3	Serchio at Piaggone	43.9299°	10.5060°	1160	24	33†	NA
4	Serchio at Filicaia	44.1360°	10.3762°	252	N.A.	NA	NA
5	Magra	44.1869°	9.9256°	947	25	20†	NA
6	Vara	44.1899°	9.8578°	555	18	6*	540*
7	Entella	44.3509°	9.3619°	297	17	7*	620*
8	Scrivia	44.7194°	8.86056°	615	57	36*	310*
9	Staffora	44.8930°	9.0569°	264	49	55*	300*
10	Trebbia	44.9089°	9.5893°	918	60	45*	400*
11	Nure	44.8816°	9.6532°	343	67	57*	310*
12	Taro	44.6976°	10.0934°	1250	63	43*	570*
13	Baganza	44.6842°	10.2130°	153	76	70*	310*
14	Parma	44.5688°	10.2370°	264	71	74*	140*
15	Enza	44.6267°	10.4133°	481	60	53*	235*
16	Secchia	44.5431°	10.767	1010	47	40*	190*
17	Panaro	44.4196°	10.925	680	38	51*	310*
18	Reno	44.3923°	11.257	990	36	28*	580*
19	Senio at Palazzuolo	44.2266°	11.632	136	25	NA	NA
20	Lamone at Biforco	44.0651°	11.601	179	21	NA	NA
21	Montone at Davadola	44.1201°	11.885	190	42	NA	NA

* Data from Garzanti et al. (1998) Ligurian Rivers (1-7) were sampled along the coastline and Adriatic Rivers (8-21) were sampled at the mountain front.

† Data from Garzanti et al. (2002). Values refer to estimates for the Massa Carrara Unit that is drained by the Magra River (5) or the Pisa Province that is drained by the Serchio River (3).

Table S2. *Sampling locations, basin area, and % catchment-averaged percent carbonate sand from this study. Lithic carbonate (Lc) point counts and average grain size for each catchment (where available) from Garzanti et al. (1998, 2002).*

Catchment Number	Catchment Name	Locality	Sample Number	Latitude	Longitude	Collection Date (dd/mm/yy)	Elevation (m)	T (°C)	pH	Ca^{2+}	K^{+}	Mg^{2+}	Na^{+}	Sr^{2+}	Si	Cl^{-}	SO_4^{2-}	HCO_3^{-}	NO_3^{-}
1	Bisenzio	Vaiano	1	43.926°	11.127°	15.07.18	118	26.0	8.84	2120.3	80.2	562.7	4483.1	5.7	133.3	1540.6	797.2	1775.0	65.1
2	Lima	Cutigliano	1	44.099°	10.752°	04.05.17	594	7.9	7.80	596.2	10.2	102.9	93.4	1.1	73.7	42.5	54.5	779.3	5.0
2	Lima	Borgo a Mozzano	1	43.999°	10.554°	15.07.18	102	24.0	8.64	1184.4	22.5	298.6	378.8	4.8	76.4	235.3	407.6	990.0	15.9
3	Serchio	Piaggione	1	43.935°	10.506°	15.07.18	51	21.2	8.14	3713.3	47.4	1317.4	1540.6	31.4	133.9	1053.1	3333.8	1175.0	43.5
4	Serchio	Filicaia	1	44.137°	10.374°	15.07.18	318	21.3	8.74	1682.8	25.2	313.9	263.7	5.7	105.4	116.2	533.9	1300.0	18.2
5	Magra	Aulla	1	44.167°	9.926°	20.03.18	55	9.9	8.19	1178.7	22.3	179.5	407.7	3.8	117.8	408.5	219.2	940.0	0.0
5	Magra	Aulla	2	44.167°	9.926°	15.07.18	28	22.5	8.42	3058.3	50.3	525.4	3314.2	14.4	74.1	2381.8	1327.3	1290.0	17.8
6	Vara	Piana Battolla	1	44.192°	9.858°	20.03.18	37	9.6	7.70	688.1	17.7	156.8	208.2	1.6	136.6	186.9	95.5	760.0	0.0
6	Vara	Piana Battolla	2	44.190°	9.858°	15.07.18	44	24.8	8.51	1165.6	25.0	365.4	357.2	2.8	119.3	179.5	132.4	1295.0	10.6
7	Entella	Carasco	1	44.351°	9.362°	20.03.18	12	9.4	8.03	752.6	13.0	158.2	188.5	1.6	96.2	185.8	78.9	680.0	0.0
7	Entella	Carasco	2	44.351°	9.362°	15.07.18	12	20.6	8.11	1171.9	27.7	254.8	655.9	2.6	117.0	305.5	98.6	1655.0	33.4
8	Scrivia	Serravalle Scrivia	1	44.719°	8.860°	18.03.18	208	7.8	8.35	1545.1	24.1	242.7	317.9	6.6	89.8	270.3	195.5	1930.0	0.0
9	Staffora	Godiasco	1	44.893°	9.057°	15.07.18	191	27.4	8.26	1409.5	70.5	721.9	837.2	10.8	254.4	265.2	419.9	1535.0	9.1
10	Trebbia	Rivergaro	1	44.908°	9.590°	22.03.18	131	4.5	8.37	1399.9	20.9	340.7	298.6	5.3	103.7	240.1	207.8	1360.0	0.0
10	Trebbia	Rivergaro	2	44.909°	9.589°	15.07.18	131	23.7	7.77	1356.6	37.4	452.9	912.7	6.7	150.2	620.3	228.1	1380.0	38.3
11	Nure	Vigolzone	1	44.882°	9.653°	21.03.18	178	7.8	8.23	1805.8	36.9	757.1	586.1	9.7	133.2	153.6	744.9	1900.0	0.0
11	Nure	Lugherzano	2	44.826°	9.617°	15.07.18	258	24.8	8.35	1442.9	44.4	753.7	492.5	6.8	199.9	114.1	294.1	1610.0	34.1
12	Taro	Ramiola	1	44.698°	10.093°	21.03.18	127	5.5	8.46	1496.9	36.5	464.6	293.6	6.3	97.1	105.3	229.6	1820.0	0.0
12	Taro	Ramiola	2	44.697°	10.094°	15.07.18	130	26.0	8.43	1403.7	56.2	565.3	529.5	6.6	136.5	144.4	242.7	1480.0	40.3
13	Baganza	Calestano	1	44.606°	10.123°	21.03.18	385	4.0	8.46	1881.2	33.4	423.4	312.2	12.7	105.4	99.4	220.9	1920.0	0.0
13	Baganza	Calestano	2	44.605°	10.120°	15.07.18	380	25.6	8.39	1253.1	42.1	504.1	681.0	12.9	123.6	253.7	338.0	1490.0	28.2
14	Parma	Pastorello	1	44.569°	10.237°	15.07.18	321	23.8	8.47	1315.0	41.0	429.5	694.2	8.8	81.3	185.1	315.3	1435.0	17.5
15	Enza	San Polo d'Enza	1	44.627°	10.413°	15.07.18	146	22.9	8.39	1473.5	58.9	560.6	868.2	8.9	88.6	235.4	434.5	1235.0	8.6
16	Secchia	Sassuolo	1	44.543°	10.767°	15.07.18	105	25.7	8.24	3944.4	99.9	875.3	1017.2	25.1	76.3	607.4	3311.5	1100.0	0.0
17	Panaro	Marano sul Panaro	1	44.420°	10.925°	15.07.18	161	24.2	8.68	1362.2	54.6	461.6	589.1	5.1	80.0	211.6	282.6	1360.0	16.5
18	Reno	Marzabotto	1	44.338°	11.213°	01.05.17	126	15.1	8.79	1182.6	27.1	326.1	425.3	3.4	35.9	166.6	245.2	1408.7	12.9
18	Reno	Scuola	1	44.362°	11.257°	03.05.17	107	17.4	8.46	1632.1	54.1	483.3	1063.5	7.7	114.5	476.2	525.5	1698.5	8.3
18	Reno	Silvano	1	44.317°	11.185°	05.05.17	145	13.8	8.46	1147.5	63.6	308.1	393.0	3.1	45.8	154.8	204.6	1448.7	8.3
18	Reno	Lentula	1	44.079°	11.051°	05.05.17	584	11.2	8.31	865.4	22.8	203.3	129.6	1.7	108.1	58.5	685.4	1109.0	5.3
18	Reno	Castello di Sambuca	1	44.104°	10.998°	05.05.17	533	11.4	8.25	871.6	91.9	220.7	156.7	1.8	223.5	80.1	126.7	1049.1	10.5
18	Reno	Poretta Terme	1	44.100°	10.962°	04.05.17	483	10.1	8.37	1054.8	16.8	240.8	147.6	2.1	84.5	55.0	119.5	1149.0	26.1
18	Reno	Limentrella di Treppio	1	44.085°	11.044°	05.05.17	518	10.5	8.34	1030.0	97.7	297.2	112.5	1.9	249.5	50.4	115.7	1198.9	9.7
19	Senio	Casola Valsenio	1	44.227°	11.632°	15.07.18	155	23.2	8.57	1424.7	85.1	1221.9	1345.1	7.9	117.5	362.7	617.2	2050.0	29.0
20	Lamone	Biforco	1	44.065°	11.601°	15.07.18	326	18.7	8.57	1468.2	55.4	860.8	743.0	9.0	129.7	169.6	353.2	1835.0	15.7
21	Montone	Dasadola	1	44.121°	11.885°	15.07.18	123	21.4	8.43	1429.5	80.4	954.5	1168.9	10.0	109.1	306.0	663.5	1680.0	29.5
21	Montone	San Benedetto	1	43.982°	11.689°	15.07.18	530	16.0	8.59	975.2	47.2	418.0	236.9	4.4	78.4	95.3	178.6	1180.0	42.2

Table S3. *Major dissolved ion concentrations and sampling location information.*

Catchment Number	Catchment Name	Locality	Sample Number	Latitude	Longitude	Bedrock Composition Correction	Date (dd.mm.yy)	Saturation Index	$[Ca^{2+}]$* (μmol/L)	$[Ca^{2+}]$* Error (μmol/L)	γ	γ (1σ)
1	Bisenzio†	Vaiano	1	43.926°	11.127°	ND	7/15/2018	1.35	ND	ND	ND	ND
2	Lima#	Cutigliano	1	43.999°	10.554°	Macigno-Cervarola	7/15/2018	0.69	3357.3	221.7	0.35	0.02
2	Lima#§	Borgo a Mozzano	1	44.099°	10.752°	Macigno-Cervarola	5/4/2017	-0.75	ND	ND	1.00	0.00
4	Serchio#	Filicaia	1	44.137°	10.374°	Macigno-Cervarola	7/15/2018	1	4055.7	261.0	0.41	0.02
5	Magra§	Aulla	1	44.187°	9.926°	External Ligurian	3/20/2018	0.01	ND	ND	1	0
6	Vara#§	Aulla	1	44.190°	9.858°	Internal Ligurian	3/20/2018	-0.78	ND	ND	1	0
6	Vara#§	Piana Battolla	2	44.192°	9.858°	Internal Ligurian	7/15/2018	0.69	ND	ND	1	0
7	Entella#§	Piana Battolla	1	44.351°	9.362°	Internal Ligurian	3/20/2018	-0.46	ND	ND	1	0
7	Entella#§	Carasco	2	44.351°	9.362°	Internal Ligurian	7/15/2018	0.33	ND	ND	1	0
8	Scrivia	Carasco	1	44.719°	8.860°	External Ligurian	3/18/2018	0.55	11531.7	610.1	0.13	0.01
9	Staffora	Serravalle Scrivia	1	44.893°	9.057°	External Ligurian	7/15/2018	0.6	15842.7	1044.4	0.09	0.01
10	Trebbia#	Godiasco	1	44.908°	9.590°	External Ligurian	3/22/2018	0.33	8706.3	480.7	0.16	0.01
10	Trebbia#§	Rivergaro	2	44.909°	9.589°	External Ligurian	7/15/2018	0.01	ND	ND	1	0
11	Nure#	Rivergaro	1	44.828°	9.617°	External Ligurian	7/15/2018	0.68	9857.5	870.1	0.12	0.01
11	Nure#	Vigolzone	1	44.882°	9.653°	External Ligurian	3/21/2018	0.46	15632.8	600.6	0.15	0.01
12	Taro#	Lugherzano	1	44.698°	10.093°	External Ligurian	3/21/2018	0.58	11140.0	566.9	0.13	0.01
12	Taro#	Ramiola	2	44.697°	10.094°	External Ligurian	7/15/2018	0.74	8923.1	585.4	0.16	0.01
13	Baganza#	Ramiola	2	44.605°	10.120°	External Ligurian	7/15/2018	0.65	15538.0	1075.0	0.08	0.01
13	Baganza#	Calestano	1	44.606°	10.123°	External Ligurian	3/21/2018	0.67	19210.0	1118.5	0.10	0.00
14	Parma#	Calestano	1	44.569°	10.237°	External Ligurian	7/15/2018	0.71	12629.7	819.3	0.10	0.01
15	Enza#	Pastorello	1	44.627°	10.413°	External Ligurian	7/15/2018	0.59	10675.5	836.3	0.14	0.01
17	Panaro	San Polo d'Enza	1	44.420°	10.925°	Macigno-Cervarola	7/15/2018	0.9	4503.3	361.7	0.30	0.02
18	Reno	Sassuolo	1	44.338°	11.213°	Macigno-Cervarola	5/1/2017	0.86	2200.3	150.3	0.54	0.03
18	Reno	Marano sul Panaro	1	44.362°	11.257°	Macigno-Cervarola	5/3/2017	0.76	5064.3	353.6	0.32	0.02
18	Reno	Marzabotto	1	44.317°	11.185°	Macigno-Cervarola	5/5/2017	0.51	1964.4	132.0	0.58	0.04
18	Reno	Scuola	1	44.079°	11.051°	Macigno-Cervarola	5/5/2017	0.09	1110.6	55.8	0.78	0.03
18	Reno#	Sibano	1	44.100°	10.962°	Macigno-Cervarola	5/4/2017	0.24	1402.8	85.6	0.75	0.04
18	Reno#	Lentula	1	44.085°	11.044°	Macigno-Cervarola	5/5/2017	0.23	1286.3	52.0	0.80	0.02
18	Reno#	Castello di Sambuca	1	44.104°	10.998°	Macigno-Cervarola	5/5/2017	0.03	1181.4	75.7	0.74	0.04
18	Reno#	Poretta Terme	1	44.183°	10.971°	Macigno-Cervarola	5/5/2017	0.91	2066.5	62.0	0.58	0.03
19	Senio#	Limentrella di Treppio	1	44.227°	11.632°	Marnoso Arenacea	7/15/2018	0.95	5553.9	336.2	0.26	0.01
20	Lamone#	Casola Valsenio	1	44.169°	11.688°	Marnoso Arenacea	7/15/2018	0.79	5670.3	306.0	0.25	0.01
20	Lamone#	Biforco	1	44.065°	11.601°	Marnoso Arenacea	7/15/2018	0.87	6775.2	345.1	0.22	0.01
21	Montone#	Davadola	1	44.121°	11.885°	Marnoso Arenacea	7/15/2018	0.71	7392.0	394.1	0.19	0.01
21	Montone#	San Benedetto	1	43.982°	11.689°	Marnoso Arenacea	7/15/2018	0.52	3385.4	167.5	0.29	0.01

#Samples used to constrain water chemistry mixing lines.

§Samples under or at saturation for which secondary calcite correction was not performed.

†Polluted sample for which additional analyses were not performed.

ND Values were not determined for these samples.

Table S4. *Saturation Index and results for secondary calcite precipitation correction.*

Catchment	Location	Latitude (°N)	Longitude (°E)	Area (km^2)	Denudation Rate (mm/yr)*	Suspended Sediment Yield ($t/km^2/yr$)*	Sediment yield (mm/yr)	Resource
Scrivia	Serravalle	44.724	8.861	605	0.035	92.7	0.08	Bartonlini et al. (1996)
Trebbia	Salvatore	44.753	9.380	631	0.118	312.7	0.28	Bartonlini et al. (1996)
Taro	S.Quirico	44.917	10.254	1476	0.412	1091.8	0.98	Bartonlini et al. (1996)
Parma	Baganzola	44.847	10.312	618	0.482	1277.3	1.15	Bartonlini et al. (1996)
Enza	Sorbolo	44.844	10.454	670	0.858	2273.7	2.04	Bartonlini et al. (1996)
Panaro	Ponte Samone	44.357	10.922	589	0.594	1574.1	1.41	Bartonlini et al. (1996)
Reno	Calvenzano	44.300	11.134	581	0.408	1081.2	0.97	Bartonlini et al. (1996)
Lamone	Sarna	44.243	11.826	261	0.627	1661.5	1.49	Bartonlini et al. (1996)
Magra	Bagni	44.198	9.951	903	0.199	526.92	0.47	Grauso et al. (2021)

*Assumes a bulk density of 2.65 t/m^3

Table S5. *Calculations of suspended sediment yield fluxes for rivers from the Northern Apennines.*

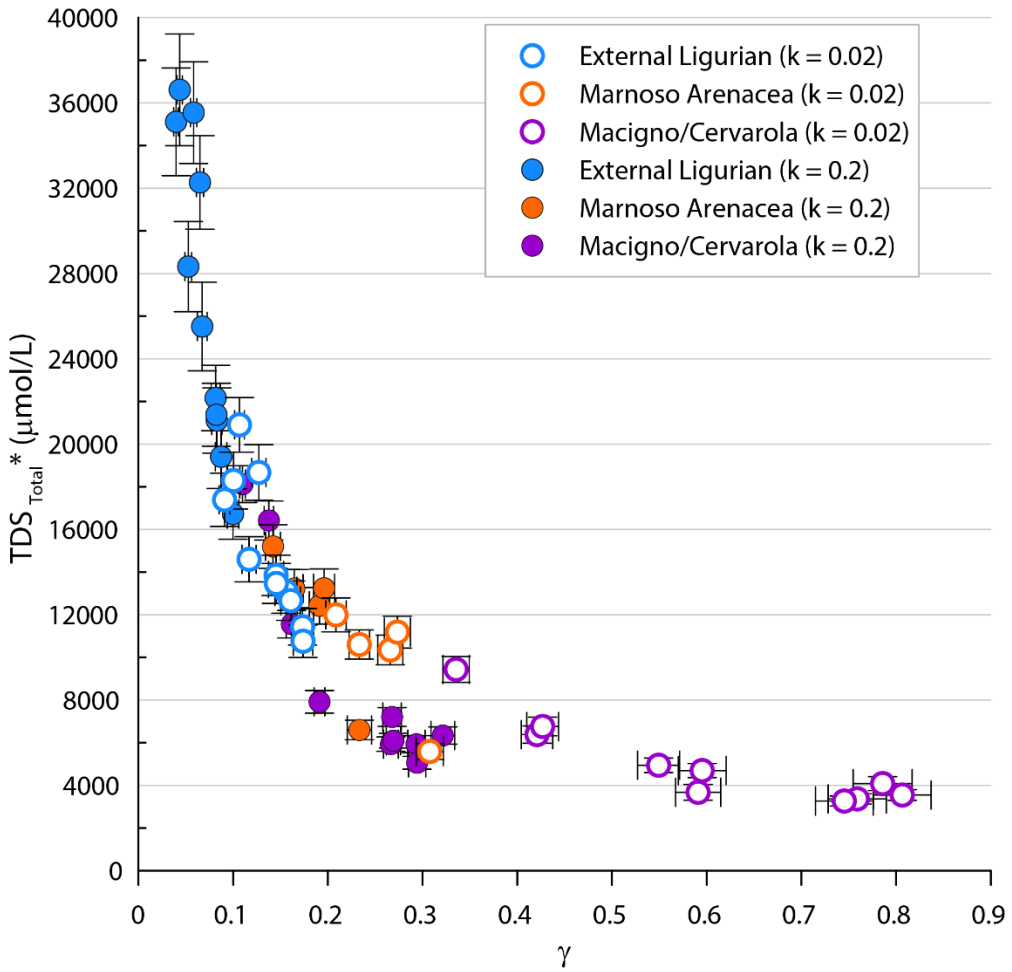

Figure S5. *Endmember corrections for secondary calcite precipitations using k = 0.02 (outlined circles) and k = 0.2 (filled circles). Internal Ligurian Unit is neglected as samples draining this unit were not corrected for secondary calcite precipitation.*

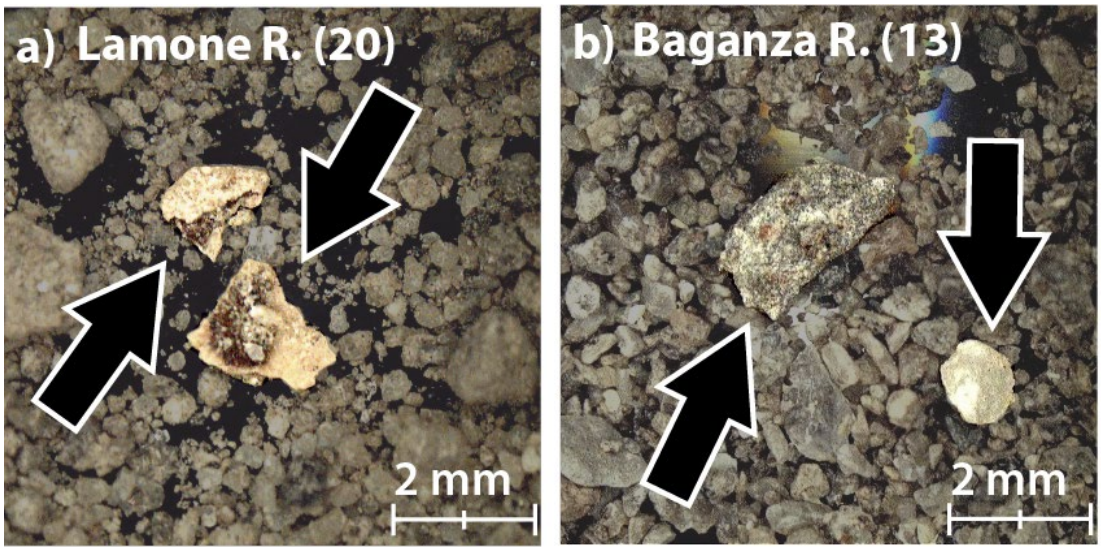

Figure S6. *Examples of carbonate grains from a) the Lamone River (River No. 20) and b) the Baganza River (River No. 13). Grains of interest are highlighted relative to the background and are indicated with arrows in each figure. a) Example of a secondary calcite grain comprised of organic matter (dark material at center of both pieces) surrounded by a carbonate crust. b) Examples of primary carbonate grains in the Baganza River. The upper-left grain is comprised of sparry micrite and the lower-right grain is a single-grain calcite.*

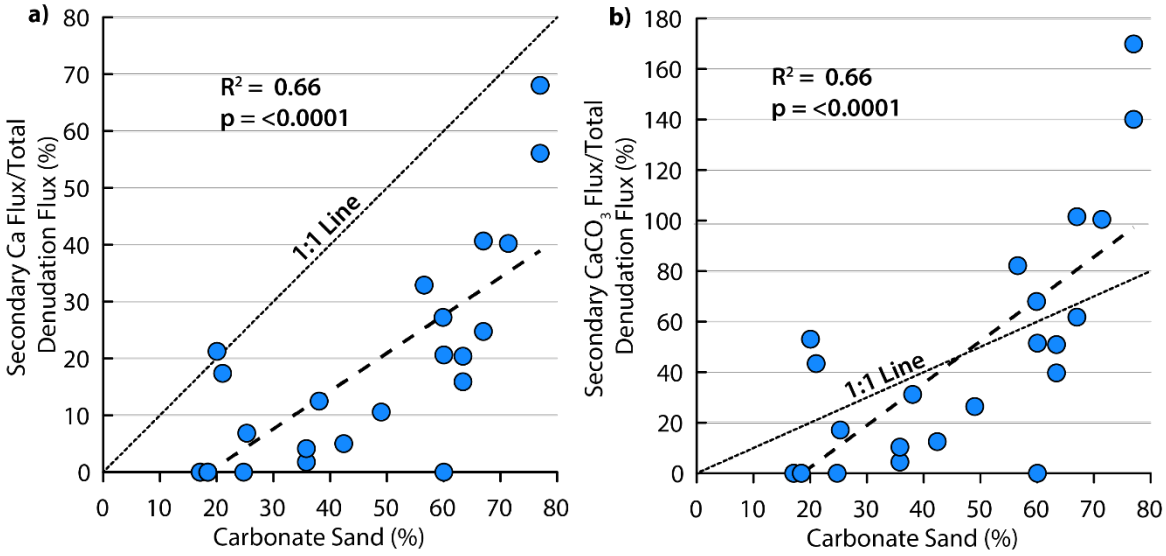

Figure S7. *Percent carbonate sand measured in catchments from this study plotted against a) the calculated secondary Ca flux as a percent of the total denudation flux and b) the calculated secondary $CaCO_3$ flux as a percent of the total denudation flux. Dotted black line represents the 1:1 line. Dashed black line represents the linear regression through the data, with associated regression statistics.*